Electronic Supplementary Material (ESI) for Nanoscale.

Supporting information

Polarity-Assisted Formation of Hollow-Frame Sheathed Nitrogen-Doped Nanofibrous Carbon for Supercapacitor

Yujiao Gong,[a] Ruyi Chen,[a] Hai Xu,[a] Chenyang Yu,[a] Xi Zhao,[a] Yue Sun,[a] Zengyu Hui,[a] Jinyuan Zhou,[c] Jianing An,[d] Zhuzhu Du,[a] Gengzhi Sun[a]* and Wei Huang[ab]*

[a]*Key Laboratory of Flexible Electronics (KLOFE) & Institute of Advanced Materials (IAM), Nanjing Tech University (NajingTech), 30 South Puzhu Road, Nanjing 211816, P. R. China*

[b]*Institute of Flexible Electronics (IFE), Northwestern Polytechnical University, 127 West Youyi Road, Xi'an 710072, P. R. China*

[c]*School of Physical Science and Technology, Lanzhou University, 222 South Tianshui Road, Lanzhou 730000, P. R. China*

[d]*School of Mechanical and Aerospace Engineering, Nanyang Technological University, 50 Nanyang Avenue, Singapore 639798, Singapore*

**Corresponding author: anjianing@ntu.edu.sg; iamgzsun@njtech.edu.cn*

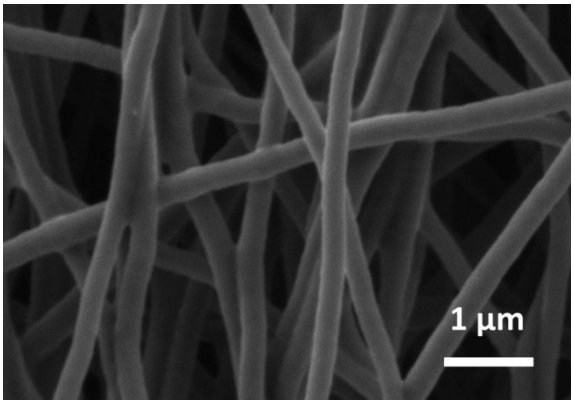

Figure S1. SEM image of CNF.

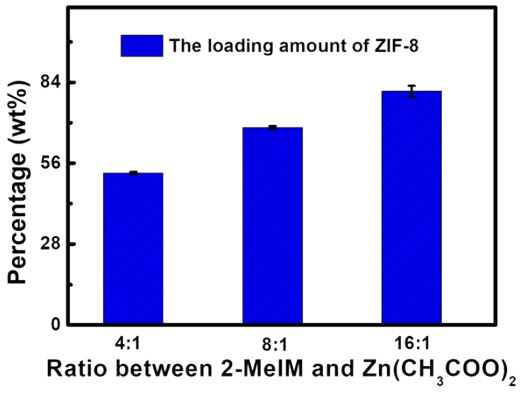

Figure S2. The loading amount of ZIF-8 obtained at different ratios between 2-MeIM and $Zn(CH_3COO)_2$.

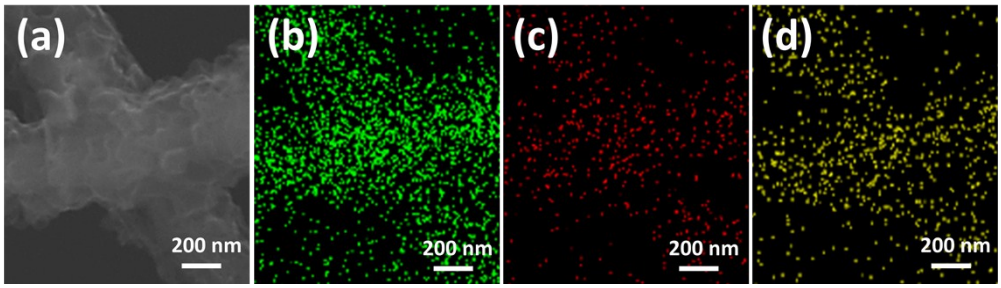

Figure S3. (a) SEM image of N-NFC-8. (b-d) EDS element mapping images of C, N, and O.

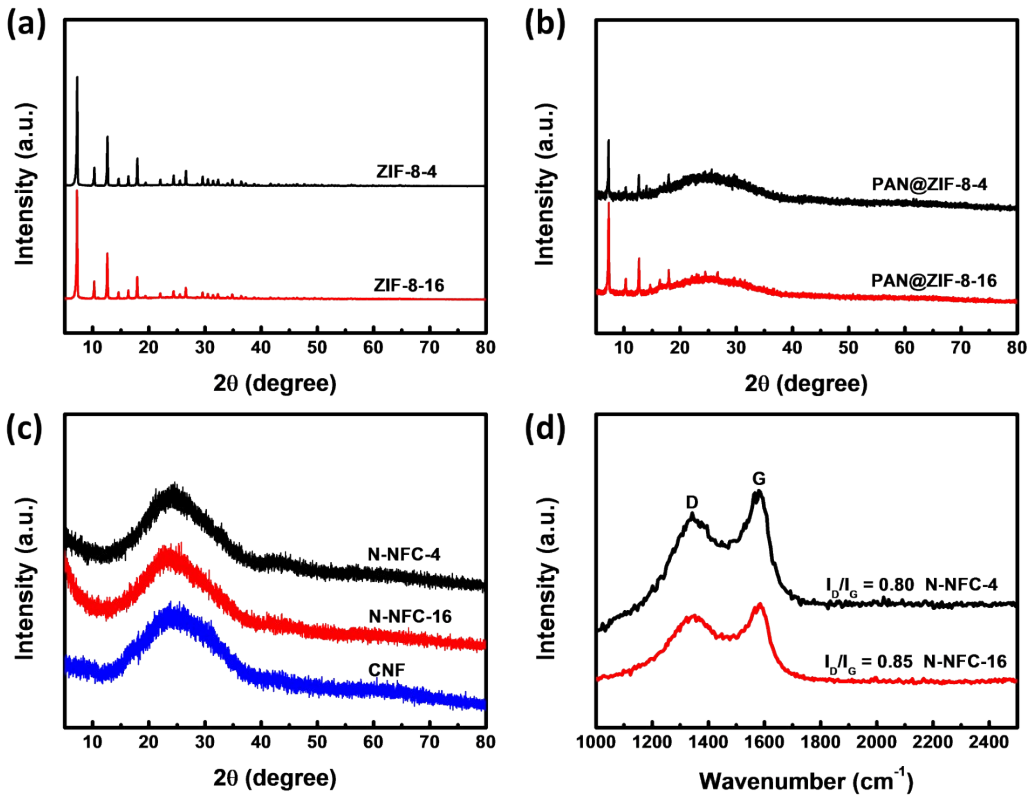

Figure S4. XRD patterns of (a) ZIF-8-4 and ZIF-8-16, (b) PAN@ZIF-8-4 and PAN@ZIF-8-16, and (c) N-NFC-4, N-NFC-16 and CNF. (d) Raman spectra of N-NFC-4 and N-NFC-16.

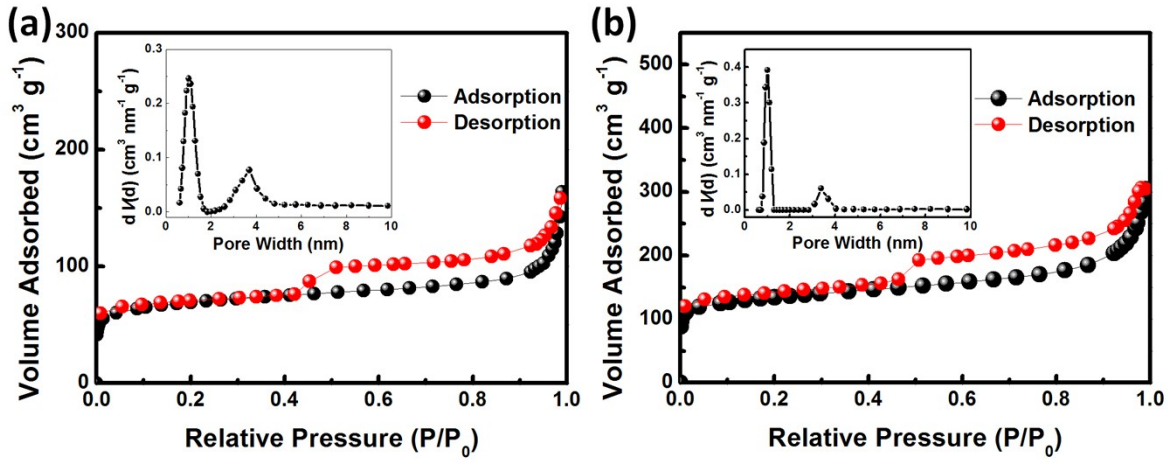

Figure S5. Nitrogen adsorption/desorption isotherms and the corresponding pore-size-distribution curves of (a) N-NFC-4 and (b) N-NFC-16.

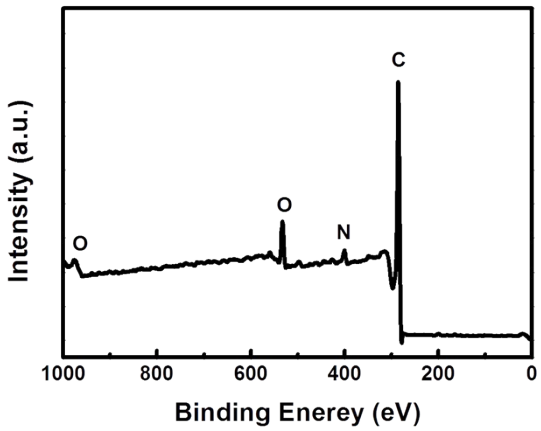

Figure S6. XPS survey of N-NFC-8.

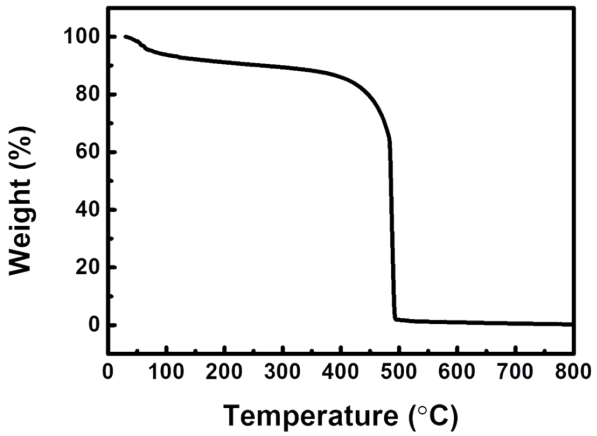

Figure S7. Thermogravimetric analysis (TGA) curve of N-NFC-8 with the ramping rates of 10°C min^{-1}.

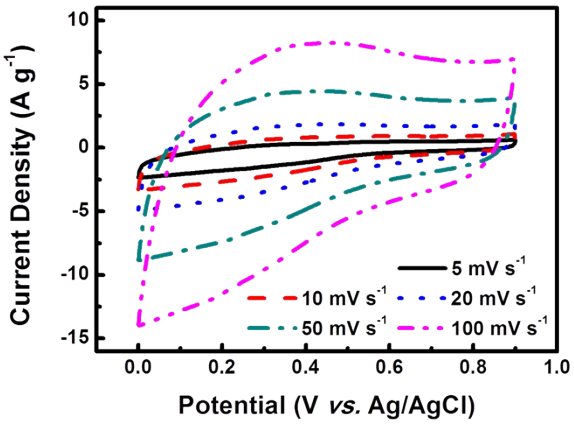

Figure S8. CV curves of CNF at different scan rates in three-electrode system.

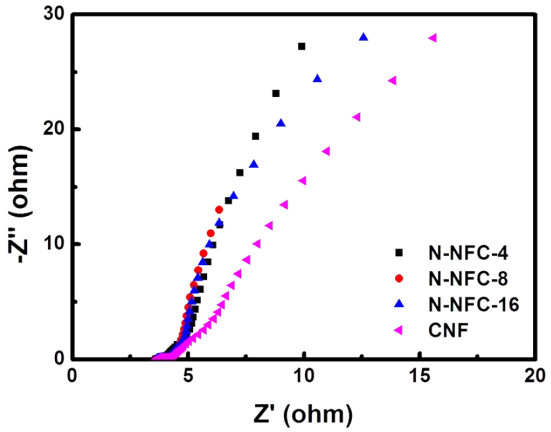

Figure S9. Nyquist plots of CNF, N-NFC-4, N-NFC-8 and N-NFC-16, respectively.

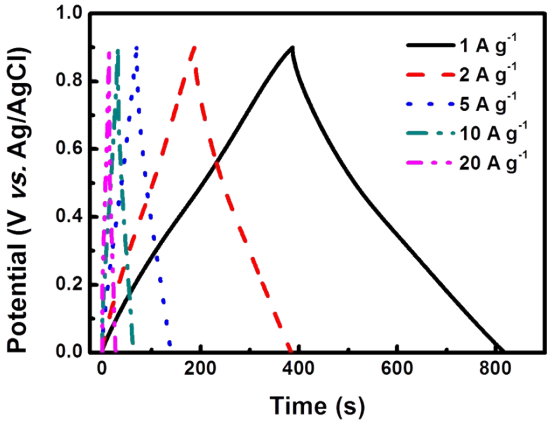

Figure S10. Galvanostatic charge-discharge curves of N-NFC-8 at different current densities in three-electrode system.

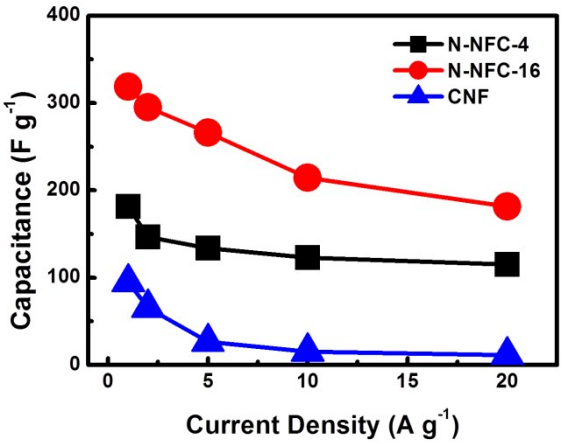

Figure S11. Rate-dependent specific capacitance of N-NFC-4, N-NFC-16 and CNF, respectively.

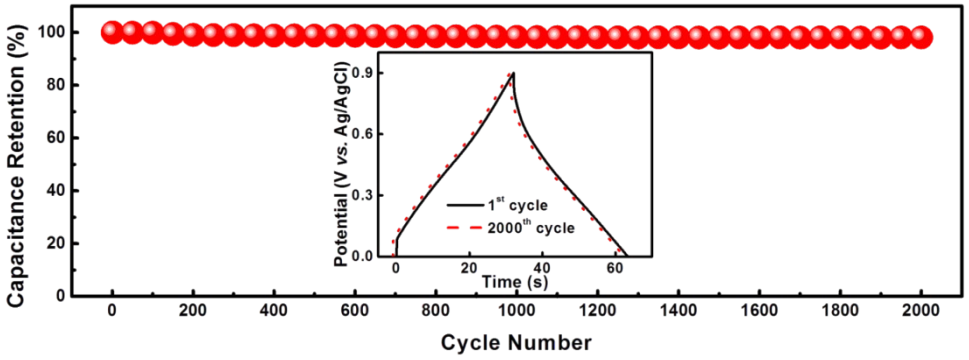

Figure S12. Cycling performance of the N-NFC-8 in 1 M H_2SO_4 at the current density of 10 A g^{-1}. Inset shows the GCD curves of the 1st and 2000th cycle.

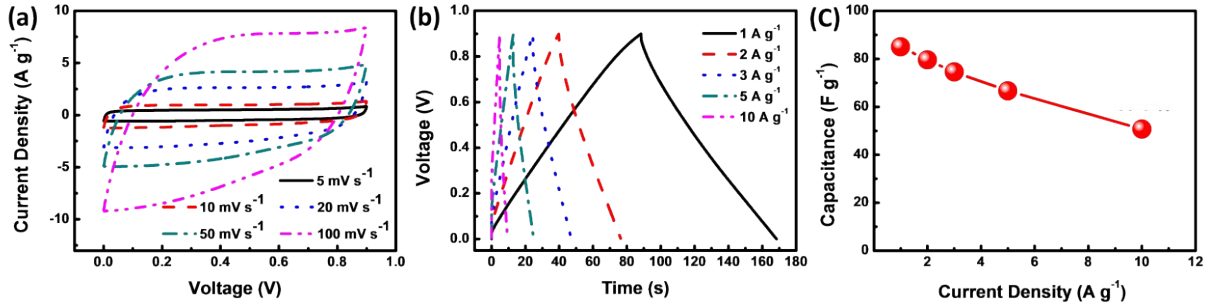

Figure S13. Two-electrode test of N-NFC-8 in 1 M H_2SO_4 electrolyte. (a) CV curves at different scan rates, (b) galvanostatic charge-discharge curves at different current densities and (c) rate-dependent specific capacitance.

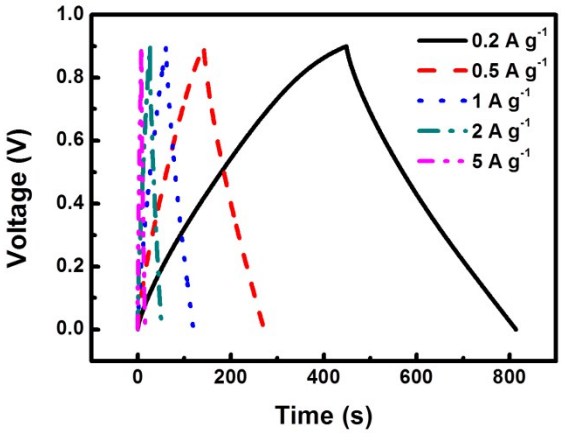

Figure S14. Galvanostatic charge-discharge curves of N-NFC-8 at different current densities in two-electrode system.